JOURNAL OF CATALYSIS 140, 1–15 (1993)

Kinetics of Methane Oxidative Coupling on Li-Doped TiO_2 Catalysts

A. M. EFSTATHIOU, D. BOUDOUVAS, N. VAMVOUKA, AND X. E. VERYKIOS

Institute of Chemical Engineering and High Temperature Chemical Processes, Department of Chemical Engineering, University of Patras, GR-26110 Patras, Greece

Received March 3, 1992; revised September 23, 1992

A kinetic study of methane conversion to C_2-hydrocarbons was conducted by cofeeding methane and oxygen at 1 bar total pressure over a series of Li-doped TiO_2 catalysts. The lithium dopant concentration was varied between 1 and 4 wt% Li_2O. Electrical conductivity measurements confirmed the incorporation of Li^+ into the crystal lattice of rutile TiO_2, XPS measurements the enrichment of the surface with lithium, and XRD the presence of Li_2TiO_3 in the 4 wt% Li_2O-doped TiO_2 catalyst. It was found that the overall activation energy for methane conversion was independent of the Li^+ dopant concentration (E = 45 kcal mol^{-1}), a result opposite to that for C_2-hydrocarbons and CO_x (x = 1, 2) formation. An optimum in methane activity was observed in the range between 0.5 and 1.5 wt% Li_2O dopant concentration. On the other hand, selectivity towards C_2-hydrocarbons showed a rather monotonic increase with Li^+ dopant concentration over a wide range of temperatures and partial pressures of methane and oxygen. The rates of C_2-hydrocarbons and CO_x formation showed dependence on Li^+ dopant concentration and also on methane/oxygen ratio. CO_2 chemisorption followed by temperature-programmed desorption was used as a probe technique to characterize the basicity of the series of Li-doped TiO_2 catalysts. It was found that the 1 wt% Li_2O-doped TiO_2 exhibited the highest amount of CO_2 uptake. A distribution in the strength of basic sites was also observed. Surface acidity measurements by amine titrations over the series of Li-doped TiO_2 catalysts revealed that total acidity decreases with increasing Li^+ dopant concentration. Surface basicity and acidity results seem to be related to the catalysis of the oxidative coupling of methane reaction over Li-doped TiO_2 catalysts.

INTRODUCTION

The partial oxidation of methane has recently become one of the most challenging problems within the scientific community, both from the fundamental as well as the practical aspect. From the fundamental point of view, the challenge is due to the high molecular stability of methane, which makes it difficult to activate the carbon–hydrogen bonds in a selective manner. From the practical point of view, methane, which is found in abundance, could function as an attractive alternative source of hydrocarbons, in view of predicted shortages in the supply of conventional oil.

A large number of materials have so far been tested for their ability to catalyze the partial oxidation of methane to higher hydrocarbons and oxygenates. These include rare-earth oxides, transition and main group metal oxides, as well as the latter oxides doped or promoted with various cations of lower or higher valence than the parent cation (*1–10*). The ultimate goal was to design a catalyst with high yields and selectivities for the desired products. The oxidative coupling of methane reaction was investigated over Li-promoted TiO_2 catalysts by Otsuka *et al.* (*11*) and Lane *et al.* (*10*). Studies related to catalyst development and mechanistic aspects of oxidative methane coupling have been examined recently (*12*), and important catalyst design parameters have been identified.

The methodology of the present work towards the development of active and selective catalysts for the partial oxidation of methane involves alteration of the electronic structure of TiO_2 (rutile) by alterva-

0021-9517/93 $5.00

lent cation doping. This involves incorporation of foreign cations into the crystal structure of TiO_2. As a result of this, the electronic structure (Fermi energy level), oxidation/reduction potential, acidity/basicity characteristics, and oxygen ion mobility are expected to be altered. These parameters are expected to influence the surface chemistry and kinetics of the reaction under investigation (*13–17*).

In the present study, kinetic results over a series of lithium-doped TiO_2 catalysts of varying dopant concentration are presented. The objective was to determine the effect of lithium dopant concentration on the kinetics of methane oxidation to C_2-hydrocarbons, and to relate this to the surface composition, and surface acidity and basicity characteristics of the catalysts. The performance of these lithium-doped TiO_2 catalysts under integral reactor conditions will be reported in a separate paper (*13*). The present results are discussed in relation to (a) previous studies on similar systems and (b) results on lattice oxygen ion mobility obtained for the present catalysts (*13*).

EXPERIMENTAL

(*a*) *Preparation of Li-Doped TiO_2 Catalysts*

Lithium-doped TiO_2 catalysts were prepared by the method of high-temperature diffusion. Lithium nitrate was used as precursor of the doping Li^+ cation in appropriate amounts so as to yield lithium concentrations in the range of 1 to 4 wt% (based on $Li_2O/(Li_2O + TiO_2)$). The precursor was mixed with TiO_2 (Degussa P-25) in a beaker containing distilled water. The slurry was heated under continuous stirring to evaporate the water, and the residue was further heated at 110°C overnight. The solid material obtained was crushed and sieved to about 48 mesh, placed in a ceramic tube, and then fired in air at 900°C for 6 h. The firing procedure involved placing the ceramic tube in a furnace and heating at a rate of 15°C/min to 900°C, maintaining at this temperature for 6 h, and then allowing to slowly cool to room temperature.

(*b*) *Characterization of Catalysts*

The Li-doped TiO_2 catalysts were characterized in terms of total surface area, their electrical conductivity and activation energy of electron conduction, their surface acidity and basicity characteristics, and their bulk and surface composition.

Total surface area was obtained following the BET method with argon adsorption at −196°C. A constant volume, high-vacuum apparatus (Micrometrics Accusorb 2100E) was used for this purpose.

Electrical conductivity experiments were performed in a flow cell under nitrogen or vacuum. The catalyst powder was compressed into a pellet of known dimensions (13 mm diam × 5 mm thickness) using a stainless steel die at a pressure of about 820 bar for 5 min. The conventional two-probe direct current technique was employed (*18*). The sample pellet was held pressed between two gold foils contacting two thin gold wires used as electrical leads and connected to a resistance meter (EICO Model 950 bridge). Resistances were recorded only when temperature was constant and conductivity did not change with time.

Surface acidities of the catalysts were measured employing the method of amine titration using Hammett indicators. The method involves titration of benzene suspensions of powdered catalysts with *n*-butylamine using Hammett indicators to determine end-points.

Selective CO_2 chemisorption followed by temperature-programmed desorption (TPD) was employed to obtain information concerning the basic sites (i.e., O^{2-}, O^-) of the catalysts. Transient chemisorption as well as TPD of CO_2 was followed by on-line mass spectrometer (Sensorlab 200D, VG-quadrupoles). Before CO_2 chemisorption the catalyst was treated with pure O_2 at 650°C for $\frac{1}{2}$ h and purged with He at the same temperature.

The surface composition of Li-doped

TiO_2 catalysts was checked by X-ray photoelectron spectroscopy (XPS). A Leybold LH 12 spectrometer was used with a hemispherical electron energy analyzer. The X-ray source used was a VSW twin anode with Mg$K\alpha$ radiation and a nonmonochromator. Measurements were taken with the sample disk kept at 100°C. The bulk composition of the Li-doped TiO_2 catalysts was checked by X-ray diffraction (XRD), employing a Siemens D 500 X-ray diffractometer with Cu$K\alpha$ radiation.

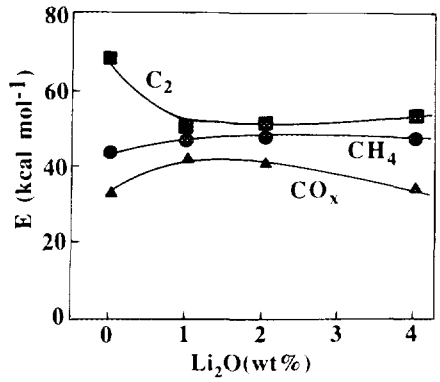

FIG. 1. Effects of Li_2O dopant concentration on the activation energy, E, of the rate of CH_4 consumption, and C_2-hydrocarbon and CO_x formation.

(c) Flow System for Kinetic, Transient, and TPD Studies

Kinetic studies were conducted in a conventional flow apparatus. This consisted of a flow measuring and control system, a mixing chamber, a fixed-bed reactor, and an online gas chromatograph (Shimadju, 9A). The flow system consists of three compressed gas cylinders, 5% CH_4/He or pure CH_4, 10% O_2/He or pure O_2, and He, which are connected to thermal mass flow meters and control valves (MKS, 247C). The flow rates of gas streams are thus monitored and controlled. The reactor is a quartz tube, 10 mm I.D., the exit of which is a quartz tube of 2 mm I.D. The catalyst particles, of an average diameter of 0.2 mm are placed near the exit tube. The reactor is encased in a furnace (Heraeus) which is controlled by a programmable temperature controller. The temperature of the catalyst bed is measured by a thermocouple placed in the middle of the bed. Separation of the effluent product stream from the reactor is performed on two packed columns, a carbosive (for separation of O_2, CO, CH_4 and CO_2) and a Poropak Q (for separation of CO_2, C_2H_4, C_2H_6, H_2O, and higher hydrocarbons). The feed and calibration gas mixtures are also analysed using a loop of a sampling valve of the gas chromatograph.

The methane conversion in all kinetic experiments presented in this work was kept between 0.9 and 1.2%. All kinetic results are reported based on 1% methane conversion after an interpolation was made between the two values, where necessary. Reaction rates are given as mol/min-m^2 based on BET surface areas.

Transient chemisorption and TPD studies of CO_2 were performed in a flow system designed as described elsewhere (*19*). The reactor used is a quartz cell of about 2.0 ml nominal volume. The amount of each catalyst sample used is 1.0 g, and the remaining empty reactor volume is filled with quartz wool. Mixtures of 1.5 and 5.0 mol% CO_2/He were used in the chemisorption studies at a flow rate of 30 ml/min (ambient).

(a) Kinetic Studies

(a.1) Effects of Li^+-dopant concentration on the activation energy and reaction order. Figure 1 shows the influence of Li^+ dopant concentration in TiO_2 on the apparent activation energy, E, of the overall CH_4 reaction rate as well as of C_2-hydrocarbon and CO_x (x = 1, 2) production rates. Table 1 gives the order of reaction with respect to CH_4 and O_2 for each doped-TiO_2 catalyst. In these studies the partial pressure of O_2 was kept constant at 0.05 bar, whereas the partial pressure of CH_4 was varied between 0.025 and 0.5 bar. Similarly, in another set of experiments the partial pressure of CH_4 was kept constant at 0.25 bar whereas the partial pressure of O_2 was varied between 0.025 and

TABLE 1

Effects of Li^+ Doping of TiO_2 on the CH_4 Coupling Reaction Order[a]

Li_2O (wt%)	X	Y
0	0.8	0.8
1	0.8	0.5
2	0.9	0.5
4	0.8	0.6

[a] Based on the rate of CH_4 consumption, $R_{CH_4} = kP^X_{CH_4} \cdot P^Y_{O_2}$.

0.3 bar. Samples were collected after 2 h on stream, the time required to obtain steady rates. A power-law rate equation of the form

$$R = A \exp(-E/RT) P^X_{CH_4} \cdot P^Y_{O_2} \quad (1)$$

is used to analyze the kinetic data.

The activation energy of the overall reaction rate (CH_4 curve, Fig. 1) is practically constant with increasing Li^+ dopant concentration (E = 45 kcal mol^{-1} between 1 and 4 wt% Li_2O). On the other hand, there is a large decrease (20 kcal mol^{-1}) in the activation energy of the reaction that leads to C_2-hydrocarbons in going from 0 to 1 wt% Li_2O dopant, but a small increase from 1 to 4 wt% Li_2O (C_2 curve, Fig. 1). An opposite behavior is obtained for the activation energy of the reaction that leads to CO and CO_2 products. In this case there is an increase by 8 kcal mol^{-1} from 0 to 1 wt% Li_2O and a decrease by 6 kcal mol^{-1} from 1 to 4 wt% Li_2O dopant concentration (CO_x curve, Fig. 1). Worth of noting is that for all the Li^+-dopant concentrations studied, the activation energy of the rate of C_2-hydrocarbon formation is higher than that of the rate of CH_4 consumption, whereas the activation energy of the rate of CO_x formation is lower. Table 1 shows that there exists a larger effect of Li^+ concentration on the reaction order with respect to O_2 reactant than with respect to CH_4 reactant.

(*a.2*) *Effect of Li^+-dopant concentration on the reaction rates and C_2-selectivity.* The influence of Li^+-dopant concentration on the overall rate of CH_4 consumption, R_{CH_4}, rate of CO_x production, R_{CO_x}, rate of C_2-hydrocarbons, R_{C_2}, and C_2 selectivity at a CH_4 partial pressure of 0.15 bar and an O_2 pressure of 0.05 bar at 750°C is shown in Fig. 2. It must be emphasized that in all cases rates were measured at the 1% methane conversion level. There is a significant increase in the rate of CH_4 consumption and C_2-hydrocarbons formation between 0 and 1 wt% Li_2O dopant, and a corresponding decrease between 1 and 2 wt% Li_2O. Note that for the latter dopant concentration, the rate of CH_4 consumption is practically the same as of the undoped TiO_2 catalyst. In addition, between 2 and 4 wt% Li_2O dopant concentration the rate of CH_4 consumption is practically constant. There is a large decrease in R_{CO_x} going from 1 to 2 wt% Li_2O; a rate smaller by a factor of 5 is obtained. On the other hand, between 2 and 4 wt% Li_2O the rate of CO_x formation increases slightly. There is a monotonic increase in the selectivity for dopant concentrations in the range 0 to 2 wt%. Further increase of dopant concentration results in a small decrease of selectivity. Similar behavior as that depicted in Fig. 2 was obtained with CH_4 pressures in the range 0.05–0.1 bar.

Figure 3 shows the effect of oxygen pressure on the rates of methane consumption,

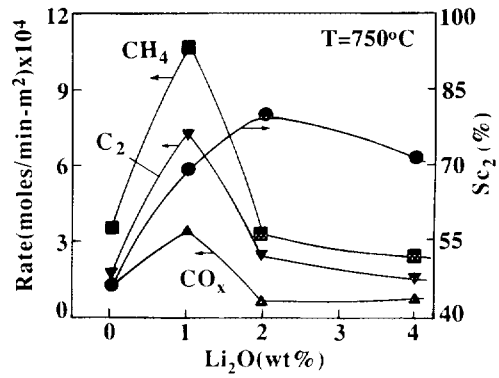

FIG. 2. Effects of Li_2O dopant concentration on the rates of CH_4 consumption, and C_2-hydrocarbon and CO_x formation, and on C_2-selectivity. T = 750°C, P_{CH_4} = 0.15 bar, and P_{O_2} = 0.05 bar.

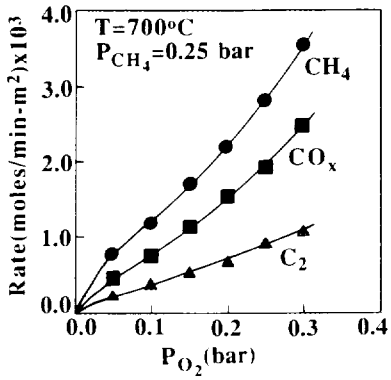

FIG. 3. Effects of oxygen partial pressure on the rates of CH_4 consumption, and C_2-hydrocarbon and CO_x formation at T = 700°C and P_{CH_4} = 0.25 bar for the 1 wt% Li_2O-doped TiO_2 catalyst.

and C_2-hydrocarbon and CO_x formation at a temperature of 700°C under a constant methane pressure of 0.25 bar for the 1 wt% Li_2O-doped TiO_2 catalyst. Similar curves were also obtained at various temperatures between 650 and 750°C, CH_4 pressurs between 0.025 and 0.15 bar, and for 2 and 4 wt% Li_2O- doped TiO_2 catalysts. A monotonic increase (almost linear) in all the rates with oxygen pressure is observed.

Figure 4 shows results of the effect of methane pressure on the rate of CH_4 consumption, and C_2-hydrocarbon and CO_x formation for the 1 wt% Li_2O-doped TiO_2 catalyst at 700°C and an oxygen pressure of 0.05 bar. All rates increase with methane pressure in a rather linear fashion. Similar behavior was obtained at 650 and 750°C.

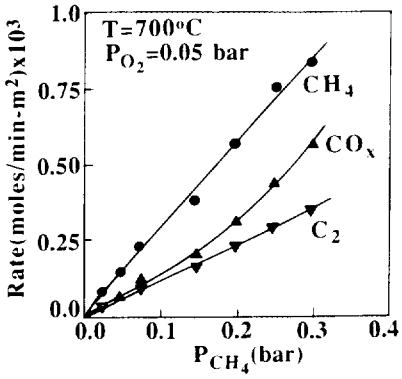

FIG. 4. Effects of methane partial pressure on the rates of CH_4 consumption, and C_2-hydrocarbon and CO_x formation at T = 700°C and P_{O_2} = 0.05 bar for the 1 wt% Li_2O-doped TiO_2 catalyst.

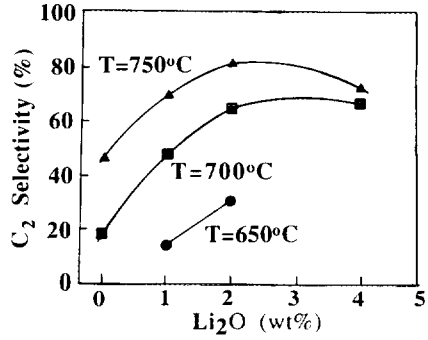

FIG. 5. Effects of Li_2O dopant concentration and temperature on C_2-hydrocarbon selectivity.

Figure 5 shows the effects of Li_2O dopant concentration on C_2 selectivity at 0.05 bar O_2 pressure and 0.15 bar CH_4 pressure for T = 650, 700, and 750°C. There is a significant increase in C_2 selectivity in the range 0 to 2 wt% Li_2O for the temperatures of 700 and 750°C. Between 2 and 4 wt% Li_2O the effects on C_2 selectivity are small. It is also observed that for all dopant concentrations studied selectivity increases with increasing temperature.

The effects of CH_4/O_2 ratio, in the range of 1.0 to 5.0, on the rates of CH_4 consumption, and CO_x and C_2-hydrocarbon formation, as observed over the 1 wt% Li_2O-doped TiO_2 catalyst at 700°C, are illustrated in Figs. 6 and 7. The results shown in Fig. 6 correspond to a constant CH_4 pressure of 0.25 bar and variable O_2 pressure between 0.05 and 0.25 bar. The results shown in Fig. 7 correspond to a constant oxygen pressure of 0.05 bar and variable CH_4 pressure, between 0.05 and 0.25 bar. It is apparent that the CH_4/O_2 ratio influences significantly the observed rates. However, at high CH_4 pressure (Fig. 6) the influence is in the opposite direction to that observed at low O_2 pressure

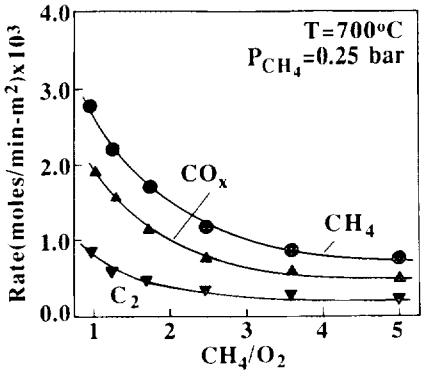

FIG. 6. Effects of CH_4/O_2 ratio on the rates of CH_4 consumption, and C_2-hydrocarbon and CO_x formation at T = 700°C and P_{CH_4} = 0.25 bar for the 1 wt% Li_2O-doped TiO_2 catalyst.

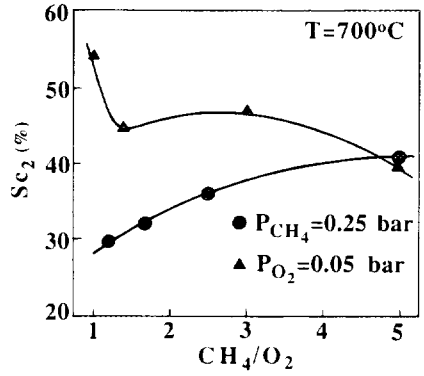

FIG. 8. Effects of CH_4/O_2 ratio on C_2-hydrocarbon selectivity at T = 700°C, P_{CH_4} = 0.25 bar, and P_{O_2} = 0.05 bar for the 1 wt% Li_2O-doped TiO_2 catalyst.

(Fig. 7). The influence of CH_4/O_2 ratio on selectivity is illustrated in Fig. 8. Here again, the directional influence of the CH_4/O_2 ratio on selectivity depends on CH_4 and O_2 partial pressures. At high CH_4 pressure, selectivity increases with increasing CH_4/O_2 ratio, while, in general, the opposite is observed at low O_2 partial pressure.

(b) Catalyst Characterization Studies

(b.1) BET surface area. BET surface area measurements for the series of Li-doped TiO_2 catalysts resulted in 0.2, 0.1, 0.2, and 0.3 m^2/g for 0, 1, 2, and 4 wt% Li_2O dopant concentrations, respectively. These results indicate that a small change in the physical area of the rutile TiO_2 occurs after the latter is doped with Li^+ at concentrations of 2 and 4 wt% and conditions described previously. However, at the 1 wt% Li_2O level of doping the specific surface area of the material is reduced to half of its original value. It should be pointed out, however, that the accuracy of the BET area measurements is not very high due to the low surface areas of the catalyst samples.

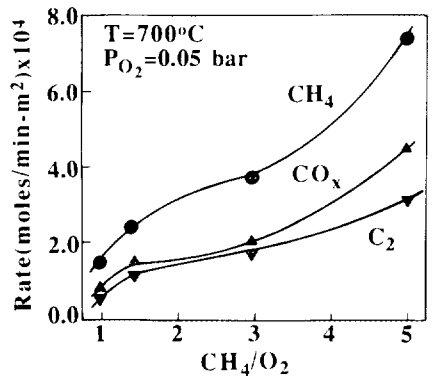

FIG. 7. Effects of CH_4/O_2 ratio on the rates of CH_4 consumption, and C_2-hydrocarbon and CO_x formation at T = 700°C and P_{O_2} = 0.05 bar for the 1 wt% Li_2O-doped TiO_2 catalyst.

(b.2) XRD and XPS measurements. X-ray diffraction studies performed on the 4 wt% Li_2O-doped TiO_2 catalyst as prepared, showed the presence of Li_2TiO_3 phase (I/I_0 = 100 at 43.7° 2θ angle). However, similar studies on the lower lithium concentration samples did not show any signal related to the Li_2TiO_3 phase. In addition, XRD patterns related to Li_2O and Li_2CO_3 phases were not observed in any of the 1–4 wt% Li_2O- doped TiO_2 catalyst samples.

The enrichment of the catalyst surface of Li-doped TiO_2 by lithium was probed by X-ray photoelectron spectroscopy measurements. The shape of the Ti (3*s*) peak with a binding energy at 61.8 eV (referenced against the Ti ($2p^{3/2}$) = 458.0 eV) prohibited the accurate measurement of lithium signal (Li (1*s*) = 54.6 eV) for the 1 and 2 wt%

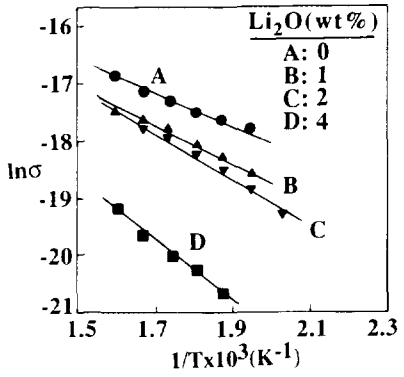

FIG. 9. Arrhenius plots of specific electrical conductivity σ for Li_2O-doped TiO_2 catalysts.

Li_2O-doped TiO_2 catalysts. It was possible to perform accurate XPS analysis only on the 4 wt% Li_2O-doped TiO_2 catalyst as prepared. The atomic ratios of Ti/O and Li/Ti are found to be 0.35 and 0.42, respectively, whereas the corresponding ratios estimated by the bulk composition are 0.47 and 0.22. For the pure TiO_2 (rutile structure) a Ti/O ratio of 0.52 was measured to be compared to the 0.50 in the bulk. It is noted that carbon (C(1*s*) = 284.4 eV) was also detected which was easily removed by sputtering. For calculating the atomic ratios mentioned above, appropriate sensitivity factors were taken from Ref. (*20*).

(*b.3*) *Electrical conductivity*. Figure 9 shows Arrhenius plots of the specific electrical conductivity, $\sigma(\Omega^{-1}\ \mathrm{cm}^{-1})$, for 0, 1, 2, and 4 wt% Li_2O dopant concentrations. The specific electrical conductivity is calculated from the expression

$$\sigma = \frac{1}{R} \cdot \frac{t}{S}, \qquad (2)$$

where R is the resistance (Ω), t is the thickness of the pellet (cm), and S is the cross-sectional area of the pellet (cm^2). The apparent activation energy of electron conduction, E_c, is calculated from the equation

$$\sigma = \sigma_0 \exp\left(-\frac{E_c}{kT}\right), \qquad (3)$$

where k is the Boltzman constant. The apparent activation energies found are 14.2, 15.4, 17.6, and 21.6 kcal mol^{-1} for 0, 1, 2, and 4 wt% Li_2O dopant concentrations, respectively.

(*b.4*) *Surface acidity and basicity*. Figure 10 gives results of the Hammett acidity function, H_0, vs the total amount of acidity (mmol/g) over the series of 0–4 wt% Li_2O doped-TiO_2 catalysts. These results are cumulative, so that each point indicates the amount of surface acidity having H_0 values equal to or less than the indicated H_0 value. It is observed that total acidity largely decreases with increasing Li_2O dopant concentration. Values of 0.008 mmol/g and 0.002 mmol/g are obtained for 0 and 1 wt% Li_2O, respectively, whereas for 2 and 4 wt% Li_2O about the same value is obtained (0.0005 mmol/g).

Surface basicity (due to surface oxygen anion sites) measurements over the Li^+-doped TiO_2 catalysts were performed employing selective CO_2 chemisorption. Figure 11 shows transient isothermal adsorption responses of CO_2 with 1 wt% Li_2O-doped TiO_2 catalyst at 35 and 150°C with 1.5 mol% CO_2/He mixture. After the O_2 pretreatment of the catalyst described previously, the reactor was cooled in He to 35 or 150°C followed by a switch to the CO_2/He mixture. The adsorption results of Fig. 11 are expressed in terms of the dimensionless quantity $Z(Z = y/y_f)$ vs time; y is the mole fraction of CO_2 in the gas phase and y_f

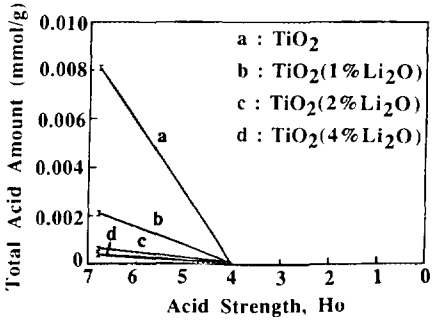

FIG. 10. Amount and strength of surface acidic sites of Li_2O-doped TiO_2 catalysts.

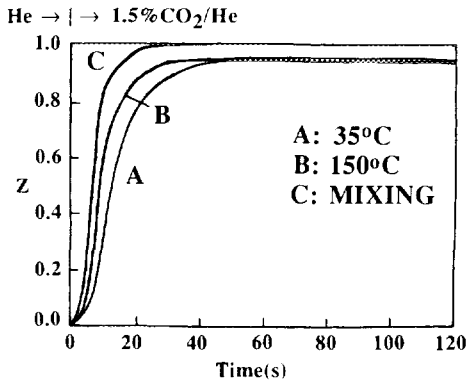

FIG. 11. Dimensionless transient response of CO_2 according to the sequence He → 1.5% CO_2/He (T, t); curve A, T = 35°C; curve B, T = 150°C. Curve C is the response of the Ar signal according to the sequence He → Ar(t).

is the mole fraction of CO_2 in the feed. The CO_2 signal was followed by on-line mass spectrometry. When the switch from He to Ar is made with simultaneous measurement of the Ar signal, curve C of Fig. 11 is obtained. This curve serves as a reference curve that allows to calculate the chemisorption amount based on the transient responses given by curves A (T = 35°C) and B (T = 150°C). More precisely, the area between the transient CO_2 response and that of curve C at a given time is proportional to the amount of CO_2 chemisorbed.

Figure 11 shows clearly that after 2 min of exposure to CO_2/He stream the approach to a steady-state value (Z = 1) is not complete. Curve A lags behind that of curve B indicating the higher uptake of CO_2 by the catalyst at 35°C than at 150°C after 2 min on stream. On the other hand, both responses show about the same Z value after 2 min of chemisorption. It was found that the Z value increases slowly towards the steady-state value (Z = 1) after 2 min on stream; about 18 h and less than 1 h are required for the CO_2 transient curves A and B, respectively, to obtain the value of Z = 1. These results probe for an activated CO_2 chemisorption process.

To further investigate the transient results of Fig. 11, CO_2 chemisorption at 35°C for various times on stream, followed by TPD, was made. These results are shown in Fig. 12a for times on stream of 2 min, 5 min, 20 min, and 18 h. The experiment was to allow a 5% CO_2/He mixture to flow over the catalyst for the indicated period of time and then to switch the feed to He for 4 min, followed by TPD (β = 20°C/min). The 4-min He treatment ensured complete purge of gas phase CO_2 before the TPD. Various features

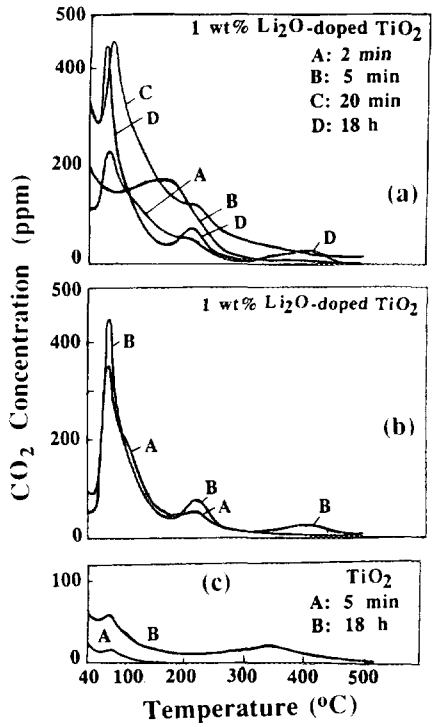

FIG. 12. (a) Temperature-programmed desorption of CO_2 on the 1 wt% Li_2O-doped TiO_2 catalyst according to the sequence He → 5% CO_2/He (35°C, Δt) → He(4 min) → TPD; curve A, Δt = 2 min; curve B, Δt = 5 min; curve C, Δt = 20 min; and curve D, Δt = 18 h. (b) Temperature-programmed desorption of CO_2 on the 1 wt% Li_2O-doped TiO_2 catalyst. Curve A, He → 5% CO_2/He (150°C, 20 min) → cool to 32°C in CO_2/He → He (4 min, 32°C) → TPD. Curve B, He → 5% CO_2/He (32°C, 18 h) → He (4 min, 32°C) → TPD. (c) Temperature-programmed desorption of CO_2 on the undoped TiO_2 catalyst. He → 5% CO_2/He (35°C, Δt) → He (4 min, 35°C) → TPD. Curve A, Δt = 5 min; curve B, Δt = 18 h.

TABLE 2

CO_2 Chemisorption on Li^+-Doped TiO_2 Catalysts at 35°C

Time of adsorption	Desorbed amount (μmol/g)		
	Isothermal (35°C)	TPD (up to 600°C)	Total
2 min	0.37	1.65	2.02
5 min	0.62	2.20	2.82
20 min	0.90	3.10	4.00
1 h	1.80	2.40	4.20
18 h	2.22	1.95	4.17

of the spectra in Fig. 12a are of interest. First, the amount of weakly adsorbed CO_2 which desorbs at 35°C (during 4-min He purge) increases with time on stream. This is indicated in Fig. 12a by the CO_2 gas phase composition at 35°C. The amount of this weakly adsorbed CO_2 is given in Table 2. Second, by increasing the time of adsorption from 2 min to 18 h (curves A–D) a second peak in the TPD spectrum appears at higher temperature (T_M = 230°C, curve D). For the case of 5 min of adsorption, no peak at around 90°C is obtained, and a rather broad spectrum is seen. For the case of 18 h of adsorption (curve D) a third peak in the TPD (T_M = 465°C) appears, whereas for smaller times of adsorption this high temperature desorbed CO_2 appeared as a tail (curves A–C). Note that no further desorption of CO_2 was found above 600°C. The amount of CO_2 chemisorption corresponding to the TPD results of Fig. 12a is given in Table 2 along with the corresponding total amount of chemisorption (isothermal desorption at 35°C plus TPD). The latter amount increases with time of chemisorption up to 1 h. The implications of this observation will be discussed later.

Figure 12b compares the TPD results obtained after chemisorption of CO_2 at 35°C for 18 h (curve B) with those after chemisorption at 150°C for 20 min followed by cooling in CO_2/He to 35°C (curve A). The latter provided 3.7 μmol/g compared to 4.17 μmol/g for curve B. Note the appearance in the TPD spectrum of the first two peaks in both cases, and that the third peak appears as a tail for the case of chemisorption at 150°C. Adsorption temperatures higher than 150°C did not provide higher amounts of chemisorption than those of Fig. 12b, curve A, upon conducting similar experiments.

Figure 12c gives TPD results for CO_2 chemisorption at 35°C for 5 min (curve A) and 18 h (curve B) on stream with the undoped rutile TiO_2. The amounts obtained are 0.03 and 0.20 μmol/g for curves A and B, respectively. These quantities are much lower than those obtained with the 1 wt% Li_2O doped TiO_2 catalyst (Table 2, Fig. 12a). CO_2 chemisorption at 150°C, as for curve A in Fig. 12b, provided an amount within 10% of that of curve B in Fig. 12c.

Similar TPD results as those of Fig. 12b were observed for the 2 and 4 wt% Li_2O-doped TiO_2 catalysts. Thus, for these two catalysts the CO_2 chemisorption at 35°C also appears to be an activated process. The quantities obtained after chemisorption at 150°C for 20 min, followed by cooling in CO_2/He to 35°C, are 0.60 and 1.15 μmol/g for the 2 and 4 wt% Li_2O dopant concentrations, respectively.

DISCUSSION

(a) *Kinetic Studies*

The effects of Li^+ dopant concentration (in the range 0–4 wt% Li_2O) in rutile TiO_2 on kinetic parameters, given in Figs. 1–8, clearly indicate the important role that surface elementary reactions play on the kinetics of CH_4 oxidation to C_2-hydrocarbons and CO_x products. Eventhough gas phase reactions may be important under certain experimental conditions (*21*), the present kinetic results strongly suggest that at least the rate-determining step(s) of the reaction is (are) influenced by the Li^+ dopant. What remains to be discussed is the actual function of Li^+ dopant concentration on the observed global reaction kinetics.

The electrical conductivity results of Fig. 9 indicate that in the present study the Li^+ cations are incorporated into the lattice of TiO_2, likely substituting lattice Ti^{4+}, and/or

at defect sites. It should be emphasized that electrical conductivity measurements were conducted with the purpose of determining whether doping of TiO_2 with Li^+ cations does indeed occur, following the procedure which was described earlier. Since electrical conductivity is a function of temperature and composition of the surrounding atmosphere, such measurements can be related to kinetic parameters and catalytic performance only if they are conducted under reaction conditions. Furthermore, such measurements should probably be conducted with more accurate techniques, such as the four-probe direct current or the two-electrode alternating current techniques (*22*, *23*).

XRD results show that Li_2TiO_3 is present in the highest concentrated Li_2O-doped TiO_2 catalyst, whereas XPS results on the latter catalyst show substantial segregation of Li from the bulk to the surface, as expected, and an increase in the ratio of O/Ti compared to that for the undoped TiO_2 catalyst. The latter implies that Li controls the surface oxygen concentration of the catalysts. The XPS results provided no evidence for the presence of Li_2O and Li_2CO_3, a result opposite to that obtained by Lane *et al.* (*10*) over 4 wt% Li_2O–TiO_2 catalyst. This difference is most likely to be due to the different method the authors employed to prepare their catalyst (*10*). Their method of catalyst preparation consisted of combining lithium oxide and rutile TiO_2 at a calcination temperature of 600°C, to be compared to 900°C calcination temperature used in the present study. It is not certain whether the 600°C calcination temperature is sufficient for doping of Li^+ to occur into the TiO_2 matrix. The O (1*s*) XPS results of the authors (Fig. 11, Ref. (*10*)) show changes in the binding energy of oxygen species with increasing lithium loading, a result not seen in the present study when comparing pure TiO_2 and 4 wt% Li_2O-doped TiO_2. These observations indicate that the catalysts used in the two studies are different. In the present case we are clearly dealing with Li-doped TiO_2, while in the case of Lane *et al.* (*10*) probably with mixed oxides of some form.

Based on the findings discussed above, it is suggested that the kinetic results presented in Figs. 1–8 must be due to effects induced by the Li^+ dopant on the active and selective centers of the catalyst surface. For instance, one could speculate that the present Li^+-doped TiO_2 catalysts have Li^+O^- centers, as reported by Lunsford and coworkers (*4*, *31*) for the Li/MgO catalyst, which may be important in generating CH_3 radicals. It must also be emphasized that alteration in bulk electronic properties, induced by incorporation of Li^+ cations into the TiO_2 matrix, also influence the electron structure of the catalyst surface which, in turn, may effect adsorptive and kinetic parameters (*16*, *17*).

Photoluminescence and TEM studies on Li^+-doped ultrafine crystalline MgO (*24*) catalyst of varying dopant concentration showed that lower coordination sites on the (111) plane did depend on Li^+ dopant concentration. This result was suggested to be related to the activity and selectivity of CH_4 coupling reaction. There is no reason to exclude the possibility that, on the present catalysts, the Li^+ dopant concentration may partly function in a similar way as the Li^+-doped MgO catalyst (*24*). The fact that a crystallographic phase of Li_2TiO_3 was found in the matrix of 4 wt% Li_2O-doped TiO_2 catalyst may be relevant to the discussion above.

Figure 1 shows that between 1 and 4 wt% Li_2O dopant concentrations the apparent activation energy for the overall CH_4 reaction rate is constant, whereas the individual reaction rates at given experimental conditions do vary with Li_2O concentration (Fig. 2). These results suggest that either the preexponential factor in the overall rate equation or the coverage of intermediates, associated with the rate-determining step(s), is influenced by the Li^+ dopant. These quantities must also depend on the surface state of the catalyst (i.e., nature of active sites).

The results of Fig. 1 strongly suggest that the carbon pathway for C_2-hydrocarbon and CO_x formation must be different, even-though the precursor intermediate species in each pathway may be the same (i.e., CH_3• species). In addition, it is very difficult to accept the idea that gas-phase reactions control the individual rates of C_2-hydrocarbon and CO_x formation, considering at the same time the large effect of Li_2O dopant concentration observed on kinetic parameters (i.e., Figs. 1 and 2).

It is very difficult from the present work to conclude about the rate-determining step(s) of the reaction system. Transient isotopic work at steady state provides the means to probe for the latter, and also to measure *in-situ* surface coverages of intermediates participating in the sequence of steps to form C_2-hydrocarbons and CO_x products (*14*, *25–30*). Based on transient isotopic results obtained for other catalysts used for the partial oxidation of CH_4 (*25*), it may be assumed here also that the rate-determining step is the abstraction of the first hydrogen atom from the CH_4 molecule by oxygen species to generate methyl radicals on the surface (*12*). Then the results of Fig. 2 may mean that the 1 wt% Li_2O concentration caused the surface coverage of adsorbed CH_4 and CH_3• species to increase with respect to the other Li_2O concentrations, and/or the activity of oxygen species towards CH_4 activation to increase.

A Li^+O^- center was suggested to be important for the process of H• abstraction from the CH_4 molecule, thus related to CH_4 activity (*31*). The activity results of Fig. 2, and others at higher conversions (*13*), along with the XRD and XPS results may suggest that an increase of Li^+ dopant concentration results in the decrease of Li^+O^- centers at the expense of formation of Li_2TiO_3, the latter not contributing to methane activation. It seems that a small concentration of lithium dopant in the range 0.5–1.5 wt% Li_2O regulates the activity of the catalyst by forming Li^+O^- centers and at the same time not blocking active sites for the formation of other adsorbed oxygen species. For the latter, it has been shown that the quantity of oxygen vacancies in the metal oxides used for the present reaction is related to the amount of dopant, and, therefore, to the amount of produced surface oxygen species, nonfully reduced (*15*).

Transient isotopic work with $^{18}O_2$ done on the present catalysts (*13*), similar to that on the Li/MgO system (*14*), provided a relation between the activation energy of bulk lattice oxygen diffusion and the Li_2O dopant concentration. A maximum in the activation energy was obtained for the 1 wt% Li_2O concentration. This result resembles that obtained for the CH_4 overall reaction rate given in Fig. 2. In addition, the basicity results with CO_2 chemisorption provided the order 1 wt% > 4 wt% > 2 wt% > 0 wt% Li_2O for the basic characteristics of the oxygen anion species of the catalysts. These results may provide a link between CH_4 activation on the surface and lattice oxygen mobility as well as basicity. The activation of CH_4 may require a stable surface oxygen anion species rather than a very mobile one. The presence of Li^+O^- centers, which were suggested to contribute to CH_4 activation as discussed previously, is related to the latter.

The behavior of the CO_x formation rate for Li_2O concentrations between 0 and 4 wt% is similar to that of R_{CH_4} and R_{C_2} (Fig. 2). Transient results of 5% CH_4/He reaction with the lattice oxygen of the present 0 and 2 wt% Li_2O-doped TiO_2 catalysts to form CO_2, to be published elsewhere, resulted in a higher activity for the latter than the former catalyst. These results may indicate (a) the role of lattice oxygen in the reaction pathway towards CO_x formation and (b) the role of Li^+ dopant loading in controlling the rate of the undesired CO_x products.

The effect of Li_2O dopant concentration on C_2-selectivity (Figs. 2 and 5), for low oxygen pressure (0.05 bar), is different from that observed on the rates of reaction (Fig. 2). Increasing the Li_2O dopant from 0 to 2 wt% results in a twofold increase in the C_2-selectivity (Fig. 2), whereas between 2 and

4 wt% Li_2O the effects are rather small. Thus, the combustion capacity of the catalysts is reduced by increasing the lithium loading. It might be suggested that increasing lithium concentration blocks lattice oxygen or oxygen vacancies active for CO_x ($x = 1, 2$) formation. There is an increase in the O/Ti ratio deduced by XPS by going from O to 4 wt% Li_2O due to the presence of Li_2TiO_3 and substitution of Ti^{4+} by Li^+. It is speculated whether Li_2TiO_3 may be responsible for blocking sites active for CO_x formation.

The higher mobility of lattice oxygen found for the 4 wt% Li_2O concentration compared to the undoped TiO_2 (*13*), and the acidity results of Fig. 10 may also be relevant to the effects of Li_2O dopant on C_2-selectivity mentioned in the previous paragraph. It is well known that acidic materials promote hydrocarbon cracking reactions. Increasing C_2-selectivities with decreasing acidity of support were reported for the same reaction system (*32*). In general, it can be stated that the effects of Li^+ dopant concentration on C_2-selectivity may be related to effects on (a) CH_4 activation to give CH_3• species on the surface (*33*, *34*), (b) coupling reaction step(s) to give C_2H_6, and (c) oxygen reaction pathway(s) to give CO_x products. Thus, a complete understanding of these issues is important in order to improve catalyst selectivity towards the C_2-hydrocarbon desired products.

Of interest are the effects of CH_4 and O_2 partial pressures on C_2-selectivity shown in Fig. 8 and on reaction rates shown in Figs. 6 and 7. The trend is that for relatively high methane partial pressures the C_2-selectivity increases and the reaction rates decrease with decreasing oxygen pressure, 0.25–0.05 bar, whereas for a relatively low oxygen pressure (0.05 bar) the C_2-selectivity decreases and the reaction rates increase with increasing methane pressure (0.05–0.25 bar). These results may at first be explained by the effect of gas phase reactions at high CH_4 and O_2 partial pressures, a result also observed with other Li-doped TiO_2 (10) and Li-doped ZnO (*35*) catalysts. On the other hand, there is a direct relation between O_2 pressure and rate of formation of surface oxygen anion species from lattice oxygen vacancies (*15*, *36*). These oxygen vacancies, as previously mentioned, are related to the Li^+ dopant concentration. Thus, gas-phase reactions with high CH_4 and O_2 pressures may not be the only reason that affects global kinetics.

The effect of temperature on C_2-selectivity is to largely increase the latter with increasing temperature (Fig. 5). This behavior was also observed for other lithium–TiO_2 catalysts (*10*) and other catalysts used for the same reaction (*32*). The present results of Fig. 1 suggest that this is due to the large differences in activation energies for C_2 and CO_x rates of formation.

The order dependence on oxygen pressure (Table 1) shows to be a strong function of Li^+ dopant concentration, a result opposite to that for the methane order dependence. In particular, for the 1 and 2 wt% Li_2O concentration the order dependence on oxygen pressure is 0.5, a result that may suggest dissociative adsorption of oxygen to generate Li^+O^- centers, whereas CH_4 adsorption seems to be of the molecular type. For the Li^+-doped La_2O_3 system (*37*), however, it was suggested that adsorption of oxygen is molecular and occurs onto anion vacancies. In addition, for the 0.18 wt% Li^+-doped ZnO system (*35*) the reaction order for CH_4 and O_2 were found to be 0.5 and 1.3, respectively, a result opposite to that obtained in the present work (Table 1).

Pure TiO_2 is an n-type semiconductor. When TiO_2 is doped with a cation of lower valence, such as Li^+, attainment of electronutrality requires generation of positive holes. Thus, the n-type semiconductivity of Li^+-doped TiO_2 is reduced, and at sufficient dopant concentration it is transformed into p-type semiconductivity. This is illustrated by the results of the activation energy of electron conduction, which clearly demonstrate that activation energy increases upon increasing Li_2O dopant concentration. It is

noted that under reaction conditions, which involve high temperatures and oxygen partial pressures, it is very likely that Li^+-doped TiO_2 exhibits p-type semiconductivity. The C_2-selectivity results of Figs. 2 and 5 that show increasing C_2 selectivity values with increasing Li_2O dopant concentration may be relevant to the transformation of n-type semiconductivity to p-type one with increasing Li_2O concentration. Other investigators (*12*) have also observed that p-type semiconductivity is essential for C_2-hydrocarbon formation.

(b) Effects of Li^+ Dopant on CO_2 Chemisorption

In the present work we have used CO_2 selective chemisorption, followed by TPD, to study the basic character of doped-TiO_2 with varying Li_2O concentration. The partial charge on the various surface oxygen anion species is taken as the parameter in determining the basicity of the present catalysts. Carbonate species, CO_3^{n-}, are expected to be formed upon CO_2 chemisorption onto the surface oxygen anions O^{n-}. It is not expected that –OH groups are present on the surface of these catalysts, considering the preparation and chemisorption conditions used.

The CO_2 TPD results of Fig. 12 have given some insight into the CO_2 chemisorption characteristics of the 1 wt% Li_2O-doped TiO_2 catalyst. First, these results strongly suggest that CO_2 chemisorption must be considered to be an activated process. There is progressively an increase in the total CO_2 chemisorption (Table 2) and a change in the relative population of at least three adsorbed states of CO_2 with increasing adsorption time up to 1 h on stream. The source of these adsorbed states may be due to several reasons.

First, one might expect some distribution of Li^+ dopant on the surface of the catalyst, which, along with some distribution of Li^+ dopant in the bulk, will produce a distribution in the effective charge of the surface oxygen anions. The XPS results reported here are consistent to this since they clearly indicate a distribution in Li^+ dopant concentration form the bulk to the surface. Second, oxygen anion species produced by interaction of gaseous oxygen and lattice oxygen vacancies may also have some distribution in their effective charge, namely different adsorbed oxygen species (i.e. O^-, O_2^- and O_2^{2-}). Such species have been reported on other metal oxides used for the same reaction (*12*, *38*). Third, transformation of a part of an initially adsorbed CO_2 state to other more energetically favorable ones may take place. The amount of weakly adsorbed CO_2 (desorbed at 35°C) given in Table 2 is relevant to the latter. It may be difficult to discriminate between the three reasons mentioned above as to which caused the observed behavior. In situ EPR and transient FTIR spectroscopies could shed some light on this matter.

The CO_2 TPD results of undoped TiO_2 (Fig. 12c) and 1 wt% Li_2O-doped TiO_2 (Figs. 12a and b) clearly demonstrate the effects of Li^+ dopant on the effective charge of the produced surface oxygen anion species. A similar spectrum in quality as that of Fig. 12c, curve B for undoped TiO_2 was also obtained for the 2 wt% Li_2O-doped TiO_2 catalyst. Thus, the significant effect of Li^+ dopant concentration on the basicity characteristics of the Li^+-doped TiO_2 catalysts can be observed. It is not easy to explain the actual behavior of Li^+ dopant concentration on the observed basicity order. It is only speculated that Li^+ dopant concentration affects the formation and stabilization of O^- species, one of the most basic oxygen species.

A distribution of basic strength, as found here, has also been reported for other basic metal oxides using CO_2 chemisorption (*39*). The present quantitative results are consistent to those reported (*39*), after considering the difference in the BET areas of the catalysts used. Finally, it is appropriate to mention that the present observed basicity order vs Li_2O dopant concentration may not be valid under reaction conditions,

where other adsorbed surface species may affect the effective charge of oxygen anion species.

CONCLUSIONS

A kinetic study on a series of lithium-doped rutile TiO_2 (0–4 wt% Li_2O) catalysts for the oxidative coupling reaction of methane revealed the following:

(a) activity for CH_4 conversion and C_2 production is highest for 1 wt% Li_2O dopant concentration. By-product CO_x activity monotonically decreases with increasing Li^+ dopant concentration in the range 1–4 wt% Li_2O, whereas C_2-selectivity increases.

(b) C_2-selectivity greatly increases with temperature for all the dopant concentrations studied. Methane and oxygen partial pressures have a strong influence on C_2-selectivity, as well as on individual reaction rates of C_2 and CO_x formation.

(c) Lattice oxygen mobility, basicity of surface oxygen anion species and surface acidity are strongly influenced by the Li^+ dopant concentration used. Their behavior with Li^+ dopant concentration seems to correlate with the present observed kinetic results.

(d) CO_2 chemisorption is found to be an activated process and strongly influenced by the Li^+ dopant concentration used. The highest amount of CO_2 chemisorption is obtained with the 1 wt% Li_2O-doped TiO_2 catalyst.

ACKNOWLEDGMENTS

Financial support by the Commission of the European Community (Contract JOUF-0044-C) is gratefully acknowledged. The authors also express their gratitude to Professor S. Ladas and E. Siokou for conducting the XPS work.

REFERENCES

1. Pitchai, P., and Klier, K., *Catal. Rev.-Sci. Eng.* **28,** 13 (1986).
2. Lee, J. S., and Oyama, S. T., *Catal. Rev.-Sci. Eng.* **30,** 249 (1988).
3. Anderson, J. R., *Appl. Catal.* **47,** 177 (1989).
4. Ito, T., Wang, J.-X., Lin, C.-H., and Lunsford, J. H., *J. Am. Chem. Soc.* **107,** 5062 (1985).
5. Deboy, J. M., and Hicks, R. F., *Ind. Eng. Chem. Res.* **27,** 1577 (1988).
6. Otsuka, K., Jinno, K., and Morikawa, A., *J. Catal.* **100,** 353 (1986).
7. Lin, C.-H., Wang, J.-X., and Lunsford, J. H., *J. Catal.* **111,** 302 (1988).
8. Taylor, P. R., and Schrader, G. L., *Ind. Eng. Chem. Res.* **30,** 1016 (1991).
9. Wang, J.-X., and Lunsford, J. H., *J. Phys. Chem.* **90,** 5883 (1986).
10. Lane, G. S., Miro, E., and Wolf, E. E., *J. Catal.* **119,** 161 (1989).
11. Otsuka, K., Liu, Q., Hatano, M., and Morikawa, A., *Chem. Lett.*, 903 (1986).
12. Dubois, J.-L., and Cameron, C. J., *Appl. Catal.* **67,** 49 (1990), and references therein.
13. Papageorgiou, D., Efstathiou, A. M., and Verykios, X. E., submitted for publication.
14. Peil, K. P., Goodwin, J. G., Jr., and Marcelin, G., *J. Catal.* **131,** 143 (1991).
15. Borchert, H., Zhang, Z. L., and Baerns, M., *in* "Amer. Chem. Soc. National Meeting, San Francisco, April 1992."
16. Akubuiro, E. C., and Verykios, X. E., *J. Catal.* **103,** 320 (1987), and references therein.
17. Akubuiro, E. C., and Verykios, X. E., *Appl. Catal.* **46,** 297 (1989).
18. Akubuiro, E. C., and Verykios, X. E., *J. Phys. Chem. Solids* **50,** 17 (1989).
19. Bennett, C. O., *in* "Catalysis under Transient Conditions" (A. T. Bell and L. L. Hegedus, Eds.), Amer. Chem. Soc. Symp. Ser., Vol. 178, p. 1. ACS, Washington, DC, 1982.
20. Briggs, D., and Seah, M. P. (Eds.), "Practical Surface Analysis," 2nd ed., Vol. 1. Wiley, New York, 1990.
21. Lane, G. S., and Wolf, E. E., *J. Catal.* **113,** 144 (1988).
22. Kiselev, V. F., and Krylov, O. V. (Eds.), "Adsorption Processes on Semiconductor and Dielectric Surfaces." Springer-Verlag, Berlin, 1985.
23. Patil, D. S., Venkatramani, N., and Rohatgi, V. K., *J. Mater. Sci.* **23,** 3367 (1988).
24. Matsuura, I., Utsumi, Y., and Doi, T., *Appl. Catal.* **47,** 299 (1989).
25. Otsuka, K., Inaidsa, M., Wada, Y., Komatsu, T., and Morikawa, A., *Chem. Lett.*, 1531 (1989).
26. Cant, N. W., Lukey, C. A., and Nelson, P. F., *J. Catal.* **124,** 336 (1990).
27. Peil, K. P., Goodwin, J. G., Jr., and Marcelin, G., *J. Am. Chem. Soc.* **112,** 6129 (1990).
28. Ekstrom, A., and Lapszewicz, J. A., *J. Phys. Chem.* **93,** 5230 (1989).
29. Mirodatos, C., Holmen, A., Mariscal, R., and Martin, G. A., *Catal. Today* **6,** 601 (1990).
30. Mirodatos, C., *Catal. Today* **9,** 83 (1991).
31. Tong, Y., Rosynek, M. P., and Lunsford, J. H., *J. Phys. Chem.* **93,** 2896 (1989).

32. Baerns, M., and Ross, J. R. H., "Perspectives in Catalysis." IUPAC Monograph, 1991, and references therein.
33. Driscoll, D. J., Martir, W., Wang, J. X., and Lunsford, J. H., *J. Am. Chem. Soc.* **107,** 58 (1985).
34. Campbell, K. D., and Lunsford, J. H., *J. Phys. Chem.* **92,** 5792 (1988).
35. Zhang, H.-S., Wang, J.-X., Driscoll, D. J., and Lunsford, J. H., *J. Catal.* **112,** 366 (1988).
36. Etsell, T. H., and Flengas, S. N., *J. Electrochem. Soc.* **116,** 771 (1969).
37. Kooh, A., Mimoun, H., and Cameron, C. J., *Catal. Today* **4,** 333 (1989).
38. Kharas, K. C. C., and Lunsford, J. H., *Prepr. Am. Chem. Soc. Div. Pet. Chem.* **35,** 200 (1990).
39. Choudhary, V. R., and Rane, V. H., *J. Catal.* **130,** 411 (1991).